

Lecture 20

Discretization Effects on Acceleration

1 Consistent Diffusion Differencing

In a previous lecture, it was shown that the diffusion-synthetic acceleration is an extremely effective means of accelerating source iterations with isotropic scattering. However, to ensure the effectiveness of the DSA method, one must discretize the transport equation in a manner that is consistent with the spatial discretization of the transport operator. This was not appreciated in early applications of the DSA method, and it led to unsatisfactory acceleration schemes. For instance, the S_n equations with diamond differencing were often accelerated using a cell-centered differencing for the diffusion operator. This approach was found to work very well in problems with scattering ratios near unity as long as the cells were optically thin. When the thickness of the cells exceeded roughly a mean-free-path, the scheme became unstable. The source of this difficulty remained a mystery until it was finally discovered during the mid 70's that consistent differencing eliminated the problem. Given spatially differenced S_n equations, the corresponding consistent diffusion equation is obtained from the S_n equations simply by using an angular Galerkin approximation based upon a linear trial space. To demonstrate the technique, let us begin with the diamond-

differenced S_n equations with isotropic scattering and an isotropic distributed source:

$$\begin{aligned} \mu_m \left(\psi_{i+\frac{1}{2},m} - \psi_{i-\frac{1}{2},m} \right) + \frac{\sigma_{t,i}}{2} \left(\psi_{i+\frac{1}{2},m} + \psi_{i-\frac{1}{2},m} \right) \Delta x_i = \\ \frac{\sigma_{s,i}}{8\pi} \left(\phi_{i+\frac{1}{2}} + \phi_{i-\frac{1}{2}} \right) \Delta x_i + \frac{q_i}{4\pi} \Delta x_i, \quad m = 1, N, \end{aligned} \quad (1)$$

Next we assume that the angular flux is linear in μ :

$$\psi_m = \frac{1}{4\pi} \phi + \frac{3}{4\pi} J \mu_m. \quad (2)$$

Next we substitute from Eq. (2) into Eq. (1), and sequentially take the zero'th and first angular moments of that equation (using the quadrature formula) to respectively obtain:

$$J_{i+\frac{1}{2}} - J_{i-\frac{1}{2}} + \frac{\sigma_{a,i}}{2} \left(\phi_{i+\frac{1}{2}} + \phi_{i-\frac{1}{2}} \right) \Delta x_i = q_i \Delta x_i, \quad (3)$$

and

$$\frac{1}{3} \left(\phi_{i+\frac{1}{2}} - \phi_{i-\frac{1}{2}} \right) + \frac{\sigma_{t,i}}{2} \left(J_{i+\frac{1}{2}} + J_{i-\frac{1}{2}} \right) \Delta x_i = 0. \quad (4)$$

We note that the properties of standard S_n quadrature sets ensures that all integrals arising in the derivation of Eqs. (3) and (4) are performed exactly. Our next task is to eliminate the currents from Eq. (3) to obtain a diffusion equation. Since for all directions,

$$\psi_i = \frac{1}{2} (\psi_{i+\frac{1}{2}} + \psi_{i-\frac{1}{2}}), \quad (5)$$

it follows that

$$J_i = \frac{1}{2} (J_{i+\frac{1}{2}} + J_{i-\frac{1}{2}}). \quad (6)$$

Using Eq. (6), we can solve Eq. (4) for the midpoint current:

$$J_i = -\frac{1}{3\sigma_{t,i}\Delta x_i} \left(\phi_{i+\frac{1}{2}} - \phi_{i-\frac{1}{2}} \right). \quad (7)$$

Next, we average Eq. (3) over cells i and $i+1$ to get:

$$\begin{aligned} \frac{1}{2} \left(J_{i+\frac{3}{2}} - J_{i-\frac{1}{2}} \right) + \frac{\sigma_{a,i+1}}{2} \left(\phi_{i+\frac{3}{2}} + \phi_{i+\frac{1}{2}} \right) \frac{\Delta x_{i+1}}{2} + \frac{\sigma_{a,i}}{2} \left(\phi_{i+\frac{1}{2}} + \phi_{i-\frac{1}{2}} \right) \frac{\Delta x_i}{2} = \\ q_{i+1} \frac{\Delta x_{i+1}}{2} + q_i \frac{\Delta x_i}{2}. \end{aligned} \quad (8)$$

Using Eq. (6), we re-express Eq. (8) as follows:

$$\begin{aligned} J_{i+1} - J_i + \frac{\sigma_{a,i+1}}{2} \left(\phi_{i+\frac{3}{2}} + \phi_{i+\frac{1}{2}} \right) \frac{\Delta x_{i+1}}{2} + \frac{\sigma_{a,i}}{2} \left(\phi_{i+\frac{1}{2}} + \phi_{i-\frac{1}{2}} \right) \frac{\Delta x_i}{2} = \\ q_{i+1} \frac{\Delta x_{i+1}}{2} + q_i \frac{\Delta x_i}{2}. \end{aligned} \quad (9)$$

Substituting from Eq. (7) into Eq. (9), we obtain the desired diffusion equation:

$$\begin{aligned} -\frac{1}{3\sigma_{t,i+1}\Delta x_{i+1}} \left(\phi_{i+\frac{3}{2}} - \phi_{i+\frac{1}{2}} \right) + \frac{1}{3\sigma_{t,i}\Delta x_i} \left(\phi_{i+\frac{1}{2}} - \phi_{i-\frac{1}{2}} \right) + \\ \frac{\sigma_{a,i+1}}{2} \left(\phi_{i+\frac{3}{2}} + \phi_{i+\frac{1}{2}} \right) \frac{\Delta x_{i+1}}{2} + \frac{\sigma_{a,i}}{2} \left(\phi_{i+\frac{1}{2}} + \phi_{i-\frac{1}{2}} \right) \frac{\Delta x_i}{2} = q_{i+1} \frac{\Delta x_{i+1}}{2} + q_i \frac{\Delta x_i}{2}. \end{aligned} \quad (10)$$

This is a three-point vertex-centered diffusion discretization that is very similar to the linear-continuous finite element scheme. To derive boundary equations, we first consider the balance equation for the left cell:

$$J_{\frac{3}{2}} - J_{\frac{1}{2}} + \frac{\sigma_{a,1}}{2} \left(\phi_{\frac{3}{2}} + \phi_{\frac{1}{2}} \right) \Delta x_1 = q_1 \Delta x_1. \quad (11)$$

Next we use Eq. (6) to eliminate $J_{\frac{3}{2}}$ from Eq. (11):

$$2 \left(J_1 - J_{\frac{1}{2}} \right) + \frac{\sigma_{a,1}}{2} \left(\phi_{\frac{3}{2}} + \phi_{\frac{1}{2}} \right) \Delta x_1 = q_1 \Delta x_1. \quad (12)$$

To proceed, we first assume (without loss of generality) a source boundary condition for the transport solution at the left boundary, and then recognize that the assumed linear dependence of the angular flux only applies to the outgoing angular flux at the boundaries.

Calculating $J_{\frac{1}{2}}$, we obtain:

$$J_{\frac{1}{2}} = \sum_{m=N/2+1}^N f_L(\mu_m) \mu_m w_m + \sum_{m=1}^{N/2} \left(\frac{1}{4\pi} \phi_{\frac{1}{2}} + \frac{3}{4\pi} J_{\frac{1}{2}} \mu_m \right) \mu_m w_m, \quad (13)$$

where $f_L(\mu_m)$ is the incident flux at the left boundary. Evaluating the integrals in Eq. (13) assuming a standard S_n quadrature set, we get

$$J_{\frac{1}{2}} = j_{in} - \frac{\langle \mu \rangle}{2} \phi_{\frac{1}{2}} + \frac{1}{2} J_{\frac{1}{2}}, \quad (14)$$

where j_{in} is the incoming half-range current

$$j_{in} = \sum_{m=N/2+1}^N f_L(\mu_m) |\mu_m| w_m, \quad (15)$$

and

$$\langle \mu \rangle = \frac{1}{2\pi} \sum_{m=n/2}^N |\mu_m| w_m. \quad (16)$$

We stress that we always define half-range currents to be positive quantities. Solving Eq. (14) for $J_{\frac{1}{2}}$, we get

$$J_{\frac{1}{2}} = -\langle \mu \rangle \phi_{\frac{1}{2}} + 2j_{in}. \quad (17)$$

This is just a Marshak source condition with the integrals evaluated via quadrature. If any other type of transport boundary condition is assumed, one similarly obtains a quadrature-generated Marshak condition of the same type. Substituting from Eq. (5) and Eq. (17) into Eq. (12), and dividing that equation by two, we get the left boundary equation for the diffusion equation:

$$-\frac{1}{3\sigma_{t,1}\Delta x_1} \left(\phi_{\frac{3}{2}} - \phi_{\frac{1}{2}} \right) + \langle \mu \rangle \phi_{\frac{1}{2}} + \frac{\sigma_{a,1}}{4} \left(\phi_{\frac{3}{2}} + \phi_{\frac{1}{2}} \right) \Delta x_1 = q_1 \frac{\Delta x_1}{2} + 2j_{in}. \quad (18)$$

The derivation of the right boundary equation is completely analogous. The resulting equation for the right boundary is

$$-\frac{1}{3\sigma_{t,I}\Delta x_I} \left(\phi_{I+\frac{1}{2}} - \phi_{I-\frac{1}{2}} \right) + \langle \mu \rangle \phi_{I+\frac{1}{2}} + \frac{\sigma_{a,I}}{4} \left(\phi_{I+\frac{1}{2}} + \phi_{I-\frac{1}{2}} \right) \Delta x_I = q_I \frac{\Delta x_I}{2} + 2j_{in} \quad (19)$$

where I is the total number of cells.

2 Discrete DSA

The discrete DSA equations with spatial diamond-differencing for the S_n equations and consistent diffusion differencing can be expressed as follows:

$$\begin{aligned} \mu \left(\psi_{i+\frac{1}{2},m}^{\ell+\frac{1}{2}} - \psi_{i-\frac{1}{2},m}^{\ell+\frac{1}{2}} \right) + \frac{\sigma_{t,i}}{2} \left(\psi_{i+\frac{1}{2},m}^{\ell+\frac{1}{2}} + \psi_{i-\frac{1}{2},m}^{\ell+\frac{1}{2}} \right) \Delta x_i = \\ \frac{\sigma_s}{8\pi} \left(\phi_{i+\frac{1}{2}}^\ell + \phi_{i-\frac{1}{2}}^\ell \right) \Delta x_i + \frac{q_i}{4\pi} \Delta x_i. \end{aligned} \quad (20a)$$

$$\phi^{\ell+\frac{1}{2}} = \sum_{m=1}^N \psi_m^{\ell+\frac{1}{2}} w_m, \quad (20b)$$

$$\begin{aligned} & -\frac{1}{3\sigma_{t,i+1}\Delta x_{i+1}} \left(\Delta\phi_{i+\frac{3}{2}}^{\ell+\frac{1}{2}} - \Delta\phi_{i+\frac{1}{2}}^{\ell+\frac{1}{2}} \right) + \frac{1}{3\sigma_{t,i}\Delta x_i} \left(\Delta\phi_{i+\frac{1}{2}}^{\ell+\frac{1}{2}} - \Delta\phi_{i-\frac{1}{2}}^{\ell+\frac{1}{2}} \right) + \\ & \frac{\sigma_{a,i+1}}{2} \left(\Delta\phi_{i+\frac{3}{2}}^{\ell+\frac{1}{2}} + \Delta\phi_{i+\frac{1}{2}}^{\ell+\frac{1}{2}} \right) \frac{\Delta x_{i+1}}{2} + \frac{\sigma_{a,i}}{2} \left(\Delta\phi_{i+\frac{1}{2}}^{\ell+\frac{1}{2}} + \Delta\phi_{i-\frac{1}{2}}^{\ell+\frac{1}{2}} \right) \frac{\Delta x_i}{2} = \\ & \frac{\sigma_{s,i+1}}{2} \left[\left(\phi_{i+\frac{3}{2}}^{\ell+\frac{1}{2}} + \phi_{i+\frac{1}{2}}^{\ell+\frac{1}{2}} \right) - \left(\phi_{i+\frac{3}{2}}^{\ell} + \phi_{i+\frac{1}{2}}^{\ell} \right) \right] \frac{\Delta x_{i+1}}{2} + \\ & \frac{\sigma_{s,i}}{2} \left[\left(\phi_{i+\frac{1}{2}}^{\ell+\frac{1}{2}} + \phi_{i-\frac{1}{2}}^{\ell+\frac{1}{2}} \right) - \left(\phi_{i+\frac{1}{2}}^{\ell} + \phi_{i-\frac{1}{2}}^{\ell} \right) \right] \frac{\Delta x_i}{2}, \end{aligned} \quad (20c)$$

$$\phi_{i\pm\frac{1}{2}}^{\ell+1} = \phi_{i\pm\frac{1}{2}}^{\ell+\frac{1}{2}} + \Delta\phi_{i\pm\frac{1}{2}}^{\ell+\frac{1}{2}}. \quad (20d)$$

We can apply a form of Fourier analysis to our discrete iteration equations. The principle is nearly identical to that of the continuous analysis. We first assume an infinite, homogeneous, uniform mesh. Next, we re-express Eqs. (20a through (20d) in terms of the errors at each step:

$$\begin{aligned} & \mu \left(\delta\psi_{i+\frac{1}{2},m}^{\ell+\frac{1}{2}} - \delta\psi_{i-\frac{1}{2},m}^{\ell+\frac{1}{2}} \right) + \frac{\sigma_t}{2} \left(\delta\psi_{i+\frac{1}{2},m}^{\ell+\frac{1}{2}} + \delta\psi_{i-\frac{1}{2},m}^{\ell+\frac{1}{2}} \right) \Delta x_i = \\ & \frac{\sigma_s}{8\pi} \left(\phi_{i+\frac{1}{2}}^{\ell} + \phi_{i-\frac{1}{2}}^{\ell} \right) \Delta x_i, \end{aligned} \quad (21)$$

$$\delta\phi^{\ell+\frac{1}{2}} = \sum_{m=1}^N \delta\psi_m^{\ell+\frac{1}{2}} w_m, \quad (22)$$

$$\begin{aligned} & -\frac{1}{3\sigma_t\Delta x} \left(\Delta\phi_{i+\frac{3}{2}}^{\ell+\frac{1}{2}} - 2\Delta\phi_{i+\frac{1}{2}}^{\ell+\frac{1}{2}} + \Delta\phi_{i-\frac{1}{2}}^{\ell+\frac{1}{2}} \right) + \frac{\sigma_a}{4} \left(\Delta\phi_{i+\frac{3}{2}}^{\ell+\frac{1}{2}} + 2\Delta\phi_{i+\frac{1}{2}}^{\ell+\frac{1}{2}} + \Delta\phi_{i-\frac{1}{2}}^{\ell+\frac{1}{2}} \right) \Delta x = \\ & \frac{\sigma_s}{4} \left[\left(\phi_{i+\frac{3}{2}}^{\ell+\frac{1}{2}} + 2\phi_{i+\frac{1}{2}}^{\ell+\frac{1}{2}} + \phi_{i-\frac{1}{2}}^{\ell+\frac{1}{2}} \right) - \left(\phi_{i+\frac{3}{2}}^{\ell} + 2\phi_{i+\frac{1}{2}}^{\ell} + \phi_{i-\frac{1}{2}}^{\ell} \right) \right] \Delta x, \end{aligned} \quad (23)$$

$$\delta\phi_{i\pm\frac{1}{2}}^{\ell+1} = \delta\phi_{i\pm\frac{1}{2}}^{\ell+\frac{1}{2}} - \Delta\phi_{i\pm\frac{1}{2}}^{\ell+\frac{1}{2}}. \quad (24)$$

We next make the fundamental assumption that the spatial dependence of the discrete angular flux error is defined by a single Fourier mode:

$$\delta\psi(x_{i\pm\frac{1}{2}}, \mu_m) = \delta\Psi_m \exp(j\lambda x_{i\pm\frac{1}{2}}), \quad (25)$$

where $j = \sqrt{-1}$. Substituting from Eq. (25) into Eq. (21), dividing that equation by $\exp(j\lambda x_i)$, and then solving for $\delta\Psi_m^{\ell+\frac{1}{2}}$, we get

$$\delta\Psi_m^{\ell+\frac{1}{2}} = \frac{\frac{\sigma_s}{4\pi} \cos\left(\frac{\lambda\Delta x}{2}\right)}{\mu_m 2j \sin\left(\frac{\lambda\Delta x}{2}\right) + \sigma_t \Delta x \cos\left(\frac{\lambda\Delta x}{2}\right)} \delta\phi^\ell. \quad (26)$$

Our next task is to obtain the scalar flux error at step $\ell + \frac{1}{2}$ in terms of the scalar flux error at step ℓ by integrating Eq. (26) over all angles using the S_n quadrature. However, rather than choose a specific quadrature order, we choose to perform the integration analytically. Multiplying both the numerator and denominator in Eq. (26) by the complex conjugate of the denominator, and integrating the resulting expression over all angles, we get:

$$\delta\Phi^{\ell+\frac{1}{2}} = \mathbf{H} \delta\Phi^\ell, \quad (27a)$$

where

$$\mathbf{H} = \frac{\sigma_s \Delta x \cos\left(\frac{\lambda\Delta x}{2}\right)}{2 \left| \sin\left(\frac{\lambda\Delta x}{2}\right) \cos\left(\frac{\lambda\Delta x}{2}\right) \right|} \arctan \left[\frac{2}{\sigma_t \Delta x} \left| \tan\left(\frac{\lambda\Delta x}{2}\right) \right| \right]. \quad (27b)$$

Note that \mathbf{H} represents the source iteration eigenfunction. Next, we make the discrete Fourier ansatz for the diffusion correction:

$$\Delta\phi_{i\pm\frac{1}{2}}^{\ell+\frac{1}{2}} = \Delta\Phi^{\ell+\frac{1}{2}} \exp(j\lambda x_{i\pm\frac{1}{2}}). \quad (28)$$

Substituting from Eqs. (27a) and (28) into Eq. (23), dividing that equation by $\exp(j\lambda x_{i+\frac{1}{2}})$, and solving for $\Delta\Phi^{\ell+\frac{1}{2}}$, we obtain the scalar flux error estimate in terms of the scalar flux error at step ℓ :

$$\Delta\Phi^{\ell+\frac{1}{2}} = \frac{\sigma_s \Delta x [1 + \cos(\lambda \Delta x)] (1 - \mathbf{H})}{\frac{4}{3\sigma_t \Delta x} [1 - \cos(\lambda \Delta x)] + \sigma_a \Delta x [1 + \cos(\lambda \Delta x)]} \delta\phi^\ell. \quad (29)$$

Finally, we substitute from Eqs. (27a) and (29) into Eq. (24) to obtain the desired eigenvalue that relates the scalar flux error at step $\ell + 1$ to the scalar flux error at step ℓ :

$$\delta\phi^{\ell+1} = \left\{ \mathbf{H} - \frac{\sigma_s \Delta x [1 + \cos(\lambda \Delta x)] (1 - \mathbf{H})}{\frac{4}{3\sigma_t \Delta x} [1 - \cos(\lambda \Delta x)] + \sigma_a \Delta x [1 + \cos(\lambda \Delta x)]} \right\} \delta\phi^\ell. \quad (30)$$

This eigenfunction has a periodic dependence upon λ . It limits to the eigenfunction for analytic DSA in the limit as $\sigma_t \Delta x \rightarrow 0$. For instance we compare the discrete source iteration and DSA eigenfunctions for $c = 1$ and $\sigma_t \delta x = 0.01$ with the corresponding analytic source iteration and DSA eigenfunctions as a function of the parameter, $\kappa = \lambda/\sigma_t$, in Fig. 1. It can be seen from Fig. 1 that the discrete and analytic eigenfunctions are essentially identical for the range of κ values considered. At larger values of κ , the eigenvalues differ from their analytic counterparts. However, given any finite range of κ values, one can always make $\sigma_t \Delta x$ small enough to obtain agreement. To demonstrate the periodic nature of discrete eigenfunctions, we plot them Fig. 2 as a function of the parameter, $\theta = \lambda \Delta_x / 2$. Two full periods of the eigenfunction are shown in Fig. 2. To demonstrate the importance of consistency in the diffusion differencing, we have computed the discrete DSA eigenfunction

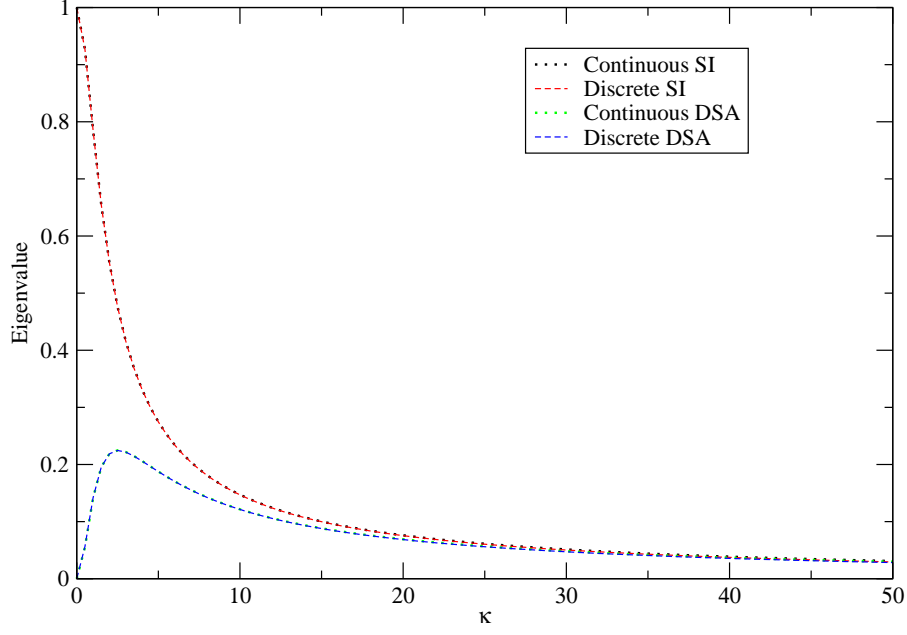


Figure 1: Comparison of discrete and analytic SI and DSA eigenvalues for $c = 1$ and $\sigma_t \Delta x = 0.01$.

after replacing the fully consistent diffusion equation Eq. (23) with the following lumped diffusion equation:

$$\begin{aligned}
 & -\frac{1}{3\sigma_t \Delta x} \left(\Delta \phi_{i+\frac{3}{2}}^{\ell+\frac{1}{2}} - 2\Delta \phi_{i+\frac{1}{2}}^{\ell+\frac{1}{2}} + \Delta \phi_{i-\frac{1}{2}}^{\ell+\frac{1}{2}} \right) + \sigma_a \Delta \phi_{i+\frac{1}{2}}^{\ell+\frac{1}{2}} \Delta x = \\
 & \sigma_s \left(\phi_{i+\frac{1}{2}}^{\ell+\frac{1}{2}} - \phi_{i+\frac{1}{2}}^{\ell} \right) \Delta x.
 \end{aligned} \tag{31}$$

The consistent and lumped DSA eigenfunctions are compared in Fig. 3 for $c = 1$ and $\sigma_t \Delta x = 0.01$. It can be seen from Fig. 3 that the eigenfunctions are essentially identical. However, we compare these two eigenfunctions for $c = 1$ and $\sigma_t = 1.25$ in Fig. 4. At this cell thickness, the consistent DSA scheme remains effective, but the lumped DSA scheme

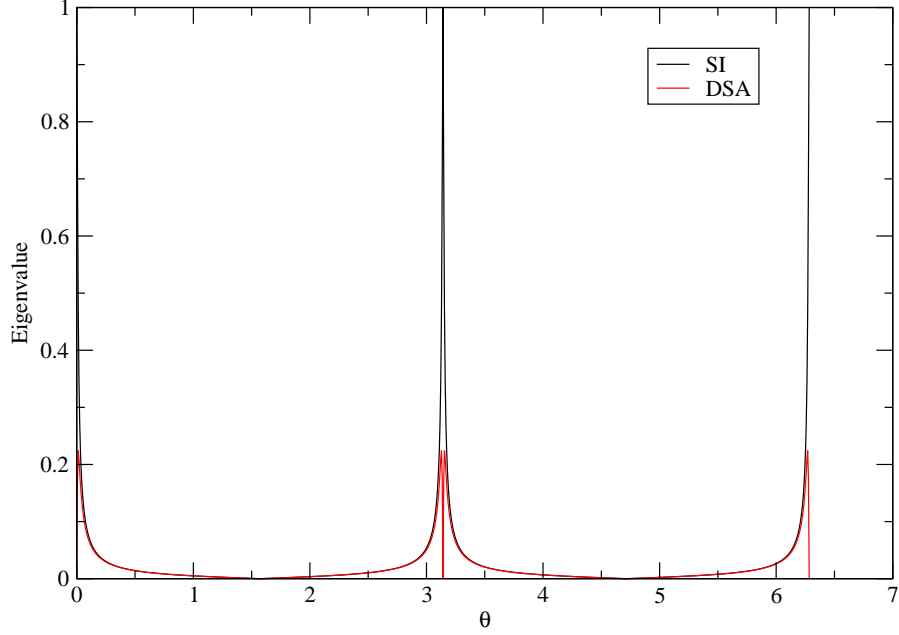


Figure 2: Discrete SI and DSA eigenvalues for $c = 1$ and $\sigma_t \Delta x = 0.01$.

is unstable with a spectral radius of about 1.2 at $\theta = \pi$. As expected the instability is associated with a high-frequency mode. It is in fact the highest-frequency mode that the mesh can support.

The consistent DSA scheme remains effective with a spectral radius of about .23 for all cell thicknesses. Some other discretizations, such as the linear-discontinuous scheme, have consistent DSA schemes that give a spectral radius of zero in the limit as $\sigma_t \Delta x \rightarrow \infty$. The lumped DSA scheme is stable at $\sigma_t \Delta x = 1.0$ but is significantly degraded with a spectral radius of roughly 0.75.

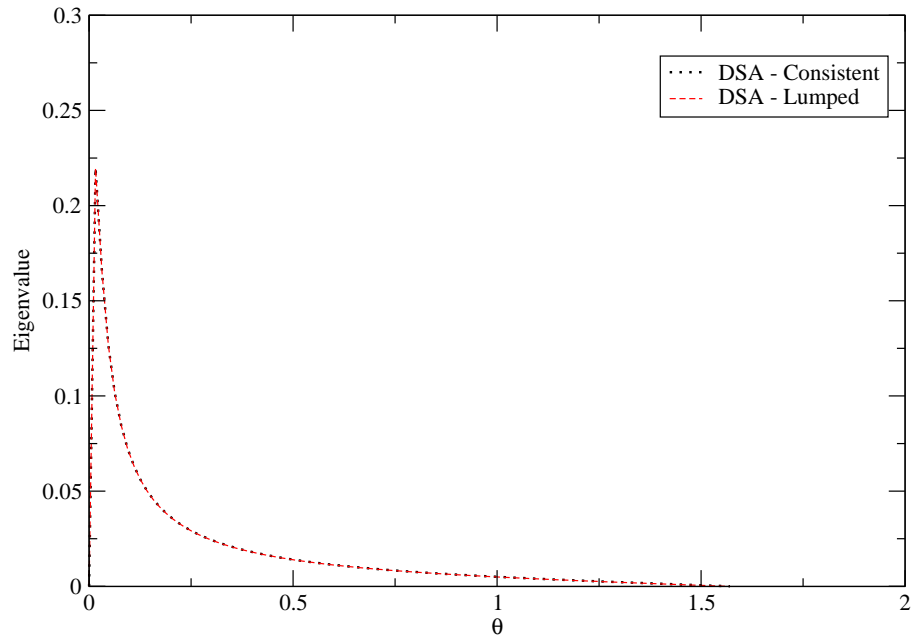


Figure 3: Comparison of Consistent and Lumped Discrete SI and DSA eigenvalues for $c = 1$ and $\sigma_t \Delta x = 0.01$.

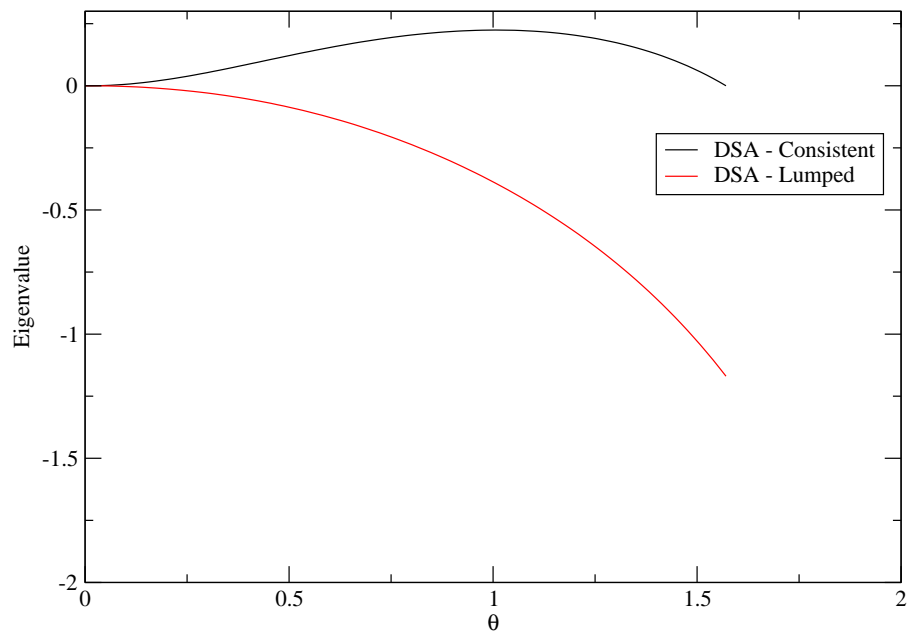


Figure 4: Comparison of Consistent and Lumped SI and DSA eigenvalues for $c = 1$ and $\sigma_t \Delta x = 1.25$.